

## Research Article

# Research on Fault Diagnosis Technology of Industrial Robot Operation Based on Deep Belief Network

Yang Shuai 

*Jiangsu Vocational College of Electronics and Information, Huaian, Jiangsu 223003, China*

Correspondence should be addressed to Yang Shuai; 044214@jsei.edu.cn

Received 14 April 2022; Revised 19 May 2022; Accepted 3 June 2022; Published 5 July 2022

Academic Editor: Lianhui Li

Copyright © 2022 Yang Shuai. This is an open access article distributed under the Creative Commons Attribution License, which permits unrestricted use, distribution, and reproduction in any medium, provided the original work is properly cited.

Fault diagnosis technology is the science of identifying the operating state of a machine or unit, and it studies the response of the change in the operating state of the machine or unit in the diagnostic information. It can give an early warning to the failure state of the machine and stop the machine before a major failure occurs so as to protect the life safety of the on-site staff and avoid huge economic losses to the enterprise. For mechanical equipment, fault diagnosis consists of three main links: fault detection; fault identification; and fault classification. Aiming at the problems that need to be solved in the fault diagnosis of industrial robots, this paper adopts a data-driven intelligent diagnosis method to establish a fault diagnosis model of industrial robots based on Deep Belief Network (DBN) and DSMT theory. Firstly, based on wavelet transform and information energy entropy correlation theory, the vibration signal of industrial robot is extracted, and the energy entropy normalized eigenvector is established. Then, the energy entropy normalized feature vector is divided into training set and test set to complete the creation of DBN network model. Finally, using DSMT theory to carry out decision-making fusion, a fault diagnosis model for industrial robots is established, and experiments are carried out on the K-R-R540 robot to verify the applicability of the established fault diagnosis model. It is proved by experiments that the industrial robot fault diagnosis model based on the deep belief network can meet the requirements of the recognition accuracy of robot faults, and the model will perform poorly when the faults coexist with multiple faults.

## 1. Introduction

The efficient production of industrial robots is the key to ensure the whole product production system of the enterprise. Therefore, enterprises and researchers pay attention to keeping industrial robots in an efficient working state. For enterprises, once the system of industrial robots breaks down, it will lead to the stagnation of the whole production line. If the faulty robot cannot be repaired in time, the robot fault may evolve into a huge production accident, and even threaten the life safety of enterprise staff. After the industrial robot is put into use, its application is under the artificial inspection and maintenance mechanism under strict regulations. The enterprise needs to invest a lot of human resources to complete the daily, weekly, and monthly inspection and maintenance of the industrial robot, and according to the inspection and maintenance record, the itinerary of the final equipment working state, and take this

as the basis to form the equipment maintenance manual of the industrial robot and summarize the equipment parameters of the industrial robot in the fault state. After data analysis, the failure frequency of each equipment, as well as the failure law and failure cause, is obtained so as to accumulate practical experience for dealing with the failure in the future. This traditional industrial robot fault diagnosis has obvious disadvantages. It needs to consume a lot of human and material resources to complete, which is unbearable for ordinary small enterprises. Because they do not have a professional enterprise maintenance team to ensure production safety, they are finally banned in the fierce market competition. Moreover, with the continuous progress of production and the uncertainty and randomness of industrial robot fault itself, it is still unable to achieve timely early warning and fault isolation for unexplained faults, which is difficult to meet the efficient and safe requirements of industrial production.

Fault diagnosis is to identify and judge the early fault characteristics of the equipment through various monitoring methods based on the operation status of the equipment so as to formulate relevant maintenance plans. Based on the above research background, this paper will take industrial robot as the research object, based on signal processing knowledge and deep learning theory, and with the help of industrial robot fault simulation platform, study the application of deep confidence network in industrial robot fault diagnosis. From the perspective of practical considerations, when the industrial robot has faults or potential faults, the research in this paper can accurately identify the fault type and judge the fault degree, provide the basis for subsequent maintenance decisions, greatly reduce the downtime, and reduce the direct and indirect economic losses. From the perspective of theoretical research, it can enrich the content of industrial robot fault diagnosis methods and provide a certain theoretical reference and basis for the development of related research work [1–10].

## 2. Related Work

The widespread use of industrial robots requires researchers to monitor and evaluate their working status in real time. In order to achieve this goal, domestic and foreign scholars and experts have done a lot of research. Freeman et al. proposed that, by analyzing the robustness of the fault cause, the corresponding filter can be designed to eliminate strong interference, and the fault diagnosis of the underwater robot can be realized by calculating the residual error of the model. Saleh Ahmad et al. established a fault diagnosis system based on a reconfigurable robot model by applying additional force and torque sensors at the joints of the robot. This method requires additional sensors to be added to the structure of the robot, resulting in the failure of the robot hardware. *Additional Charges*. Hashimoto et al. established a fault diagnosis model based on Bayesian time series by analyzing the failure causes of the robot under working conditions, which can quickly identify the occurrence of robot faults and isolate them. This method requires a large number of system parameters of robot faults as prior conditions to guarantee the accuracy of the model. Verma et al. established a robot fault diagnosis method based on discrete-time observer by designing an observer method and completed the fault diagnosis of robot joints through the cooperation of detection and diagnosis observers. This method requires a large amount of joint sensor information. Jaber et al. analyzed the fault signals of the robot under various working conditions by collecting the vibration signal of the working state of the robot, using wavelet transform, time-frequency domain analysis, and other methods to realize the fault diagnosis of the robot. Ferreira et al. used the synovial observer to establish a robot fault diagnosis model and applied it to the fault diagnosis of the COMAU robot. The experiment proved that this method can achieve accurate diagnosis for a single fault, but it does not perform well in the diagnosis of robot fault states with multiple faults coexisting. The safe operation of industrial robots requires maintenance personnel to complete the processing of the

faults that have occurred or will occur in time. The traditional fault diagnosis methods have been unable to adapt to the current production mode of enterprises. The establishment of a fault diagnosis model suitable for industrial robots is to solve this problem. Due to the complex structure of industrial robots, concurrent failures often occur. It is precisely because of the existence of this problem that a fault diagnosis method for industrial robots based on analytical thinking logic has been proposed. By using the idea of deep learning, it is possible to explore and identify the intrinsic relationship between various types of faults in industrial robots. So that when the robot fails, it can easily solve the failure problem in the operation of the industrial robot [11–15].

## 3. Related Theoretical Methods

*3.1. Failure Analysis of Industrial Robots.* The failure forms of industrial robots usually manifest as control system failures and drive system failures. Therefore, industrial robot failures can be divided into two categories: logical failures and physical failures. Logical faults are mainly caused by the failure of the industrial robot control system, and the robot cannot complete tasks according to the instructions, which is mainly manifested in the decline of performance indicators; physical faults are mainly due to the robot shutdown caused by the hardware failure of the industrial robot, including circuit aging or damage, motor failure, bearing wear, and reducer failure. Table 1 shows several common failure forms, failure characterizations, and failure causes of industrial robots. It can be seen from Table 1 that there is not a simple one-to-one correspondence between the failure forms of industrial robots, the failure representations, and the failure causes. Some more complex failure forms and failure representations correspond to multiple failure causes, and some failure causes will also occur. There are many different forms of failure characterization. Since the failure of industrial robots will be accompanied by changes in vibration signals, and it is precisely because of this unique feature, the easiest way to evaluate the current working state of industrial robots is to judge the vibration signals of industrial robots. According to the basis, as well as having good applicability, using vibration signal as the fault of industrial robot is also used as a main research method to study the fault of industrial robot [16].

### 3.2. Deep Belief Networks

*3.2.1. Restricted Boltzmann Machines.* Ordinary Boltzmann Machine (BM) is the predecessor of RBM. Each BM structure consists of two layers of networks, which are defined as the visible layer  $v$  and the hidden layer  $h$ , respectively. Figure 1 shows the BM structure. It can be found that the network structure of BM is fully connected by random neurons, so it has a strong ability to learn specific rules from complex data in an unsupervised form, but at the same time its disadvantages are also obvious. The fully connected structure makes the network. The training time is long, and the computational cost is high. The emergence of

TABLE 1: Several common failure forms, failure characterizations, and failure causes of industrial robots.

Failure form	Fault characterization	Cause of issue
Power system failure	The robot cannot be powered on	Power circuit failure
	Robot cannot move	Power chip failure
	The host computer restarts	Short circuited
Control system failure	Controller cannot be powered	Damaged control chip
	The control port is unstable	Control chip soldering
		Controller failure
	Robot out of control	Control program run away
		Damaged control chip
Drive joint failure	Motor failure	Motor stuck
		Driver chip failure
		Motor overcurrent protection
	Bearing failure	Bearing wear
	Bearing fracture	
	Reducer failure	Damaged reducer
		Coupling loose

RBM is to improve the defects of BM network structure; it is a new unsupervised learning network structure model based on greedy learning. Except for the undirected nature of the interlayer connection, there is no difference from the general BM principle in terms of network definition of each layer, neuron output and representation, and neuron state value rules. Figure 2 shows the RBM structure organization. The energy model of RBM can be intuitively understood as follows: a small ball with a rough surface and an irregular shape is placed anywhere in a large bowl with a very rough surface. Affected by gravitational potential energy, generally speaking, when the state is stable, the probability of the ball staying at the bottom of the bowl is the greatest, and of course there is a certain possibility that it will stay at other positions in the bowl. In the theory of the energy model, the final stable stop position of the ball is defined as a state, each state corresponds to an energy, and this energy can be represented by an energy function. So, in a sense, the probability that the ball is in a certain state can be expressed by the energy of the ball in the current state [17].

3.2.2. *Basic Structure of Deep Belief Network.* RBM is an important foundation of DBN. From the macroscopic point of view, the network structure of DBN is mainly composed of several RBM stacks and a labeled classifier, as shown in Figure 3. As can be seen from Figure 3, this deep DBN network has four layers of hidden units, the input of the network is the sample data that meets the requirements, and the top is the label information corresponding to the input data. First, the prepared input sample data is assigned to each neuron in the visual layer of the first layer one by one, after a series of iterative training and learning (i.e., forward greedy learning and backward fine-tuning; the specific process will be introduced later), the weight matrix between each layer and the bias value of each neuron will reach a certain stable state, which can fit the training samples to the maximum extent. After the training is completed, when a test data sample is input, the trained network will automatically analyze and process the data and assign the possibility of each category according to the calculation

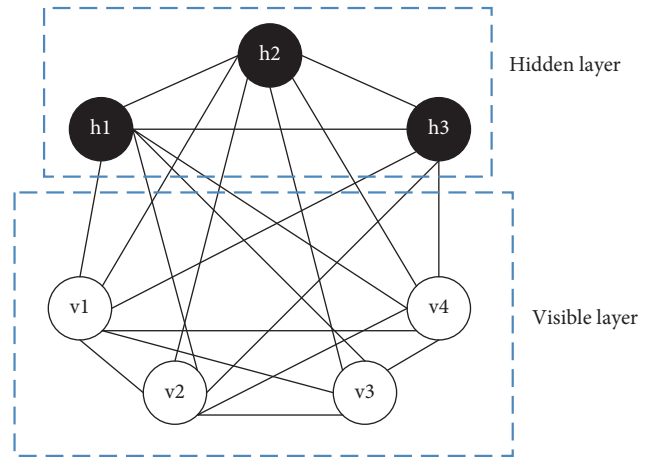


FIGURE 1: Schematic diagram of BM structure.

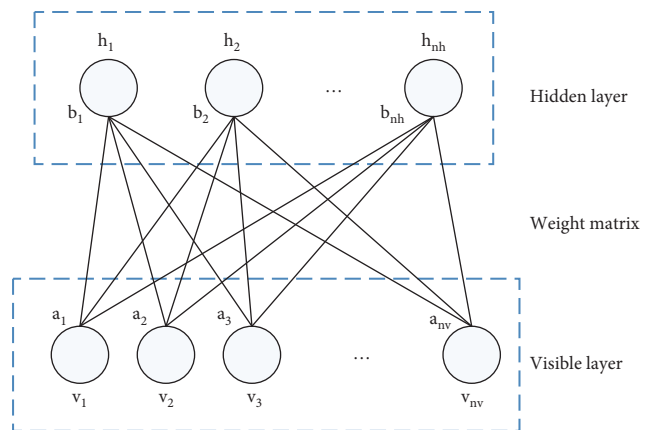


FIGURE 2: Basic structure of RBM.

result, and the sample will be included in the corresponding category with the highest probability. Inside the network, all feature data can share the entire network information together. This sharing mode makes it more convenient to extract the deep features of the data and can significantly enhance the memory capacity of the entire network. The

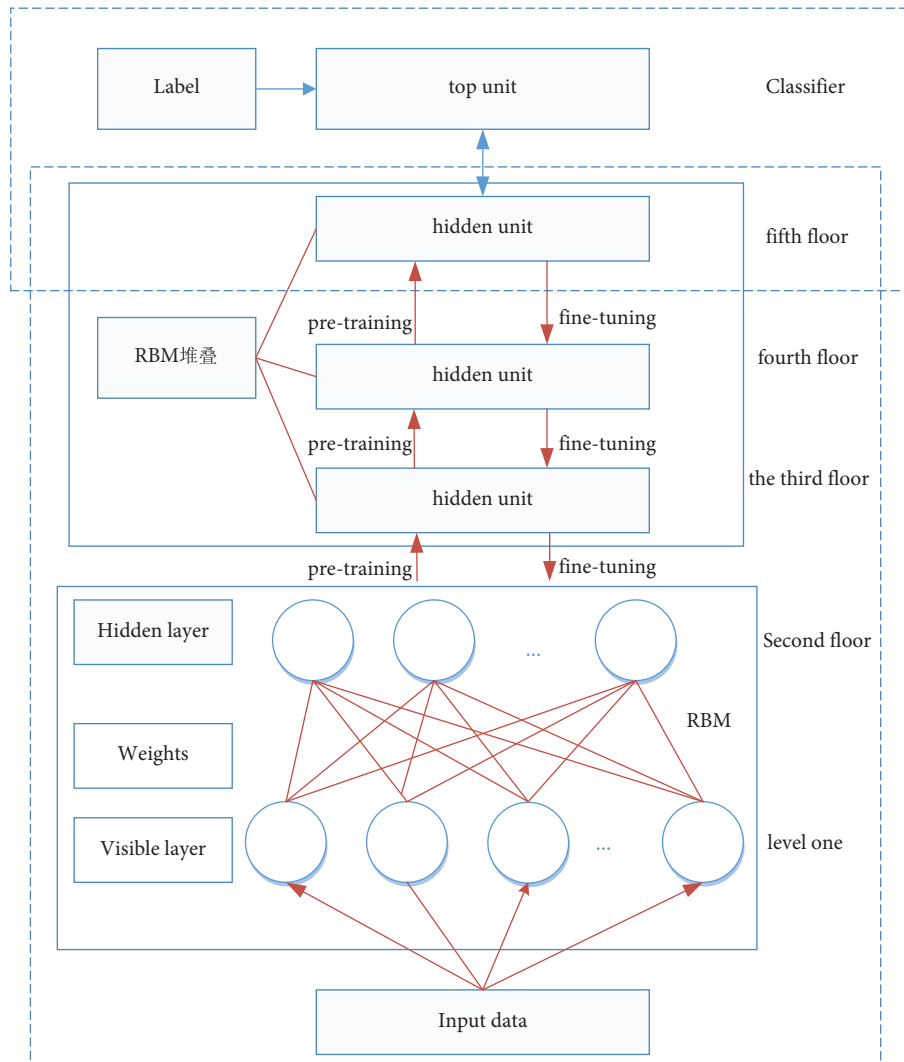


FIGURE 3: Schematic diagram of DBN network structure.

training process of DBN mainly includes two processes: forward greedy learning and backward fine-tuning. The greedy learning process of RBM is mainly to extract and mine the feature information of the input data layer by layer, and the backward fine-tuning process is to fine-tune the structural parameters of the entire DBN network through the known labels so as to adjust the parameters in the deep layer containing multiple hidden layer parameter vectors [18]. Through the neuron of the deep belief network and the ability to extract and mine the feature information of the input data layer by layer, it has a good application performance in industrial robot diagnosis.

**3.2.3. Forward Greedy Learning.** The forward greedy learning process is also called stacked RBM pretraining. In the whole process, the algorithm itself learns the data without the participation of label information, which belongs to a category of unsupervised learning. Before the DBN algorithm was proposed, one of the main bottlenecks encountered by the BP neural network was that when the number of network layers

was too large, the problem of gradient dispersion would occur during the training process, resulting in a poor learning effect of the entire model. The proposed unsupervised greedy learning method solves this problem, it divides the deep network into multiple shallow network structures and restricts model training and parameter adjustment to this shallow networks, good training results for the entire model can be achieved. The forward greedy learning process is shown in Figure 4. As can be seen from Figure 4, the training in each step is completed within a certain RBM. In the first step, the input data is assigned to the neurons of the visual layer, the data of the visual layer  $v$  is mapped to the hidden layer  $h_1$  through greedy learning, and then the hidden layer  $h_1$  is reconstructed through the CD-k algorithm to return to the hidden layer. View layer, and adjust the internal weights and biases after calculating the reconstruction error. On the basis of the first step, use the fully trained parameter vector to solve the hidden layer  $h_1$ , and use it as the input of the second RBM structure, and train the subsequent RBM structure in the same way until the training of the entire DBN network is completed [19–21].

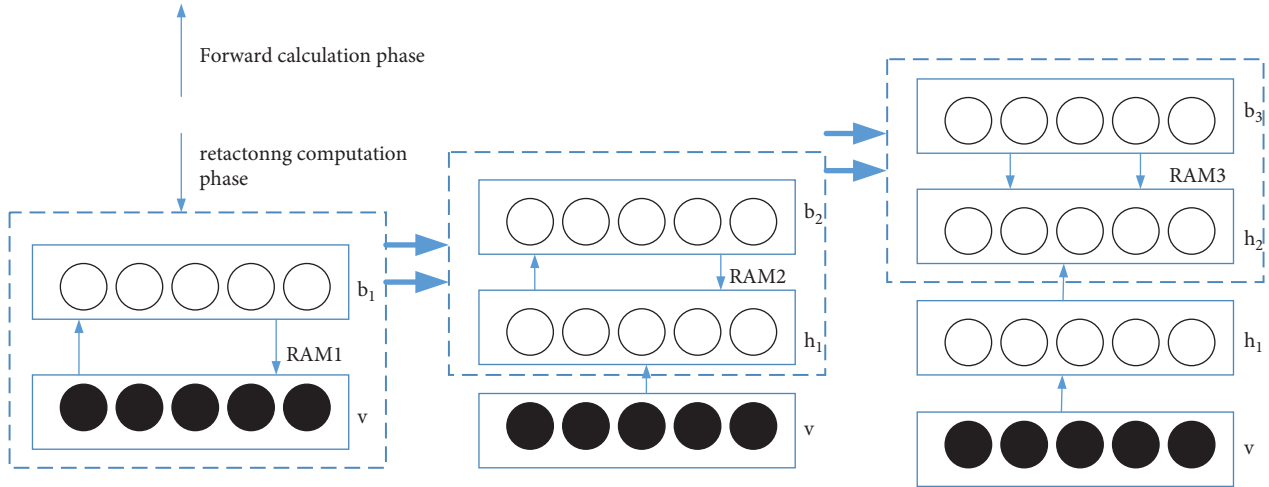


FIGURE 4: Greedy learning process before and after.

3.2.4. *Backward Fine-Tuning.* Forward greedy learning is a typical unsupervised training process, which can roughly capture information on the input vector, that is, obtain a solution set within a large range, and the corresponding internal parameter vector of each RBM is initially determined, but the model cannot be obtained. For a high-precision optimal solution, so it is necessary to use the backward fine-tuning strategy to find it from this large-scale solution set. Different from the forward greedy learning, the backward fine-tuning process is a supervised learning method. The pretrained parameters are used as initialization parameters, and the label information is used to further optimize each layer of the DBN network to improve the overall recognition rate and enhancement of the DBN network. *Robustness of the Model.* The principle of DBN's backward fine-tuning algorithm is similar to that of BP's reverse adjustment, mainly including fast gradient descent method and conjugate gradient descent method. Compared with the model obtained by the BP algorithm alone, the performance of the model after fine-tuning the network as a whole by using the gradient descent method combined with the label information tends to be better. Because the pretraining step has been performed before fine-tuning, it is now equivalent to only needing to do a local search within a specific parameter space, so it is relatively easier to converge, and it takes less time. The reverse fine-tuning process is shown in Figure 5.

## 4. The Establishment of Four Major Industrial Robot Fault Diagnosis Experimental Platforms

### 4.1. Introduction to the Experimental Platform

4.1.1. *Experimental Equipment.* The experimental platform is designed with the KR-3-R540 robot as the main equipment. The experimental equipment mainly includes KR-3-R540 robot, vibration exciter, several acceleration sensors, data acquisition and storage system, and data analysis system. Among them, the data acquisition and storage system and the data analysis system together constitute the

experimental host computer, which can realize the calling and analysis of the vibration signal through the computer and obtain the experimental results; since the fault used in this chapter is described as the fault at the joint of the robot, the vibration excitation is used. The controller applies a preset continuous excitation at the robot joints, in this way to simulate the failure of the robot joints. The data analysis system is a computer equipped with Modal Genius software provided by Yiheng Company, the operating system is Windows 10, the CPU is Intel Core i7, and the running memory is 16 G.

4.1.2. *Experimental Platform Function.* In order to realize the acquisition of the vibration signal of the KR-3-R540 robot joint and the end effector, the main functions of the experimental platform designed in this chapter are as follows: (1) Acceleration sensor is used to collect the vibration signal of the acceleration sensor, of which a single acceleration sensor can only collect the vibration signal on the Z-axis; the three acceleration sensors can collect the vibration signal in the three directions of XYZ and store it in the data acquisition and storage system, which is convenient for the computer to retrieve the vibration data of the robot joints at any time. This system is Hangzhou Yiheng, the sensor data acquisition and storage system provided by the company. (2) Through the KR-3-R540 robot teach pendant, change the trajectory of the robot and the running speed of the robot (resp., 30%, 50%, and 70% of the maximum speed) so that the acceleration sensor can collect data at different speeds and different working trajectories. The robot vibration signal provides data support for model creation. (3) Through the modal analysis software, the modal analysis of the robot is carried out through the modal test. Through modal analysis, determine the cut-off frequency of the robot resonance frequency and vibration frequency. Provide data support for designing filter parameters in the next step. Figure 6 shows the sensor layout of the KR-3-R540 robot. A single acceleration sensor is applied from joint 1 to joint 5, corresponding to sensor 1 to sensor 5, respectively; because the structure of the end effector

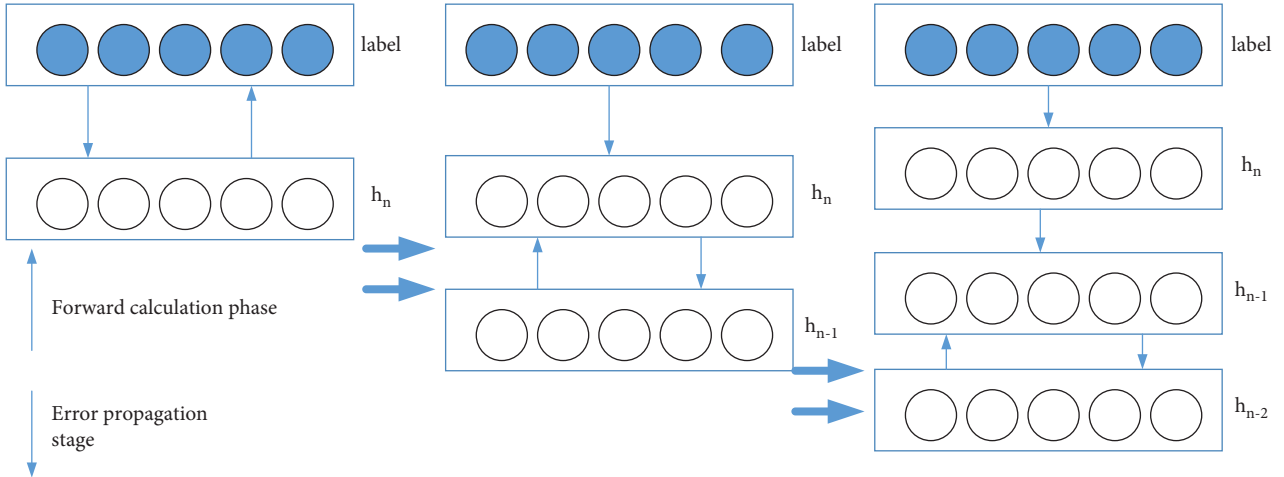


FIGURE 5: Background fine-tuning process.

and joint 6 is close, it is only at the end. Three acceleration sensors are applied to the actuator, corresponding to sensor 6, and no acceleration sensor is added to joint 6. Figure 6 shows the schematic diagram of the experimental platform. The vibration data is transmitted to the data acquisition and storage system through the single acceleration sensor applied to the robot joint and the three acceleration sensors of the end effector, and the subsequent analysis is performed by the computer.

#### 4.2. Experiment Content and Data Collection

**4.2.1. Experiment Content.** Due to the interference of the motion frequency and resonance frequency of the robot, there is a large error in the original signal of the sensor. The range of the motion frequency and resonance frequency of the robot is obtained through the modal analysis experiment, and the signal is filtered by designing a filter. The time length is divided into experimental samples to obtain experimental data sets. In order to realize the creation of the robot fault diagnosis model, it is necessary to design experiments to collect the response joint vibration signals. Due to the limitation of technology and cost, the robot failure state used in this section is described as the robot's end pose deviation, which is not within the allowable range. The fault is a fault at the joint, and the fault is in the form of a simulated fault. The vibration exciter is set to continuously excite and interfere with the joint motion of the robot, resulting in the deviation of the robot's end pose beyond the allowable range. Set the robot running trajectory as a straight line in space. As shown in Figure 7, the vibration exciter interferes with the movement trajectory of the robot end effector before and after joint 1. In Figure 7(a), the movement trajectory of the robot end effector is in normal state; Figure 7(b) is the motion trajectory of the robot end effector after the vibration exciter interference (the point where the maximum deviation is intercepted is enlarged and displayed, and the different colors in the figure represent the repetitive motion trajectory of the robot). Since the error range of the robot's end effector is  $[0, 0.35 \text{ mm}]$ , comparing Figures 7(a)

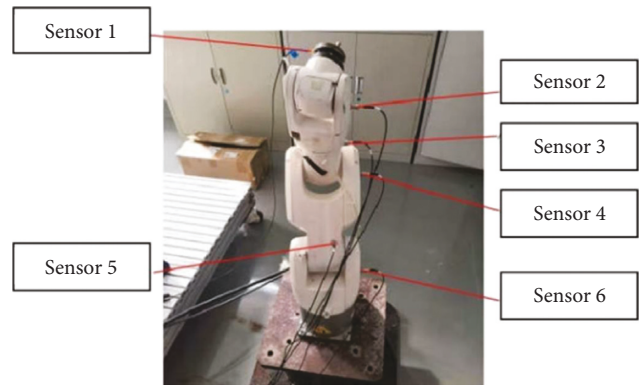
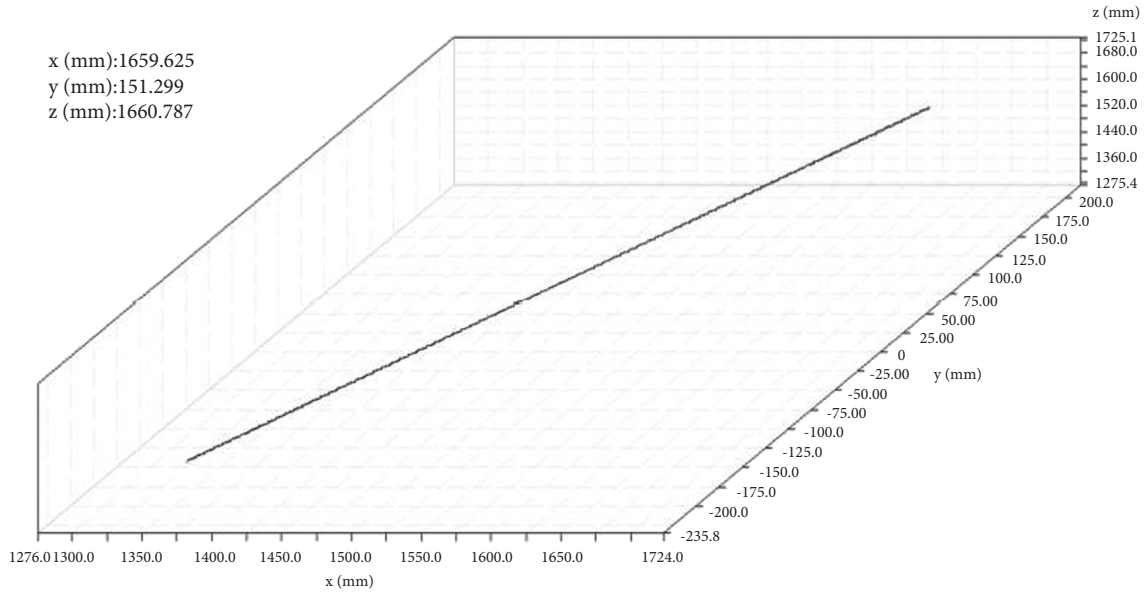


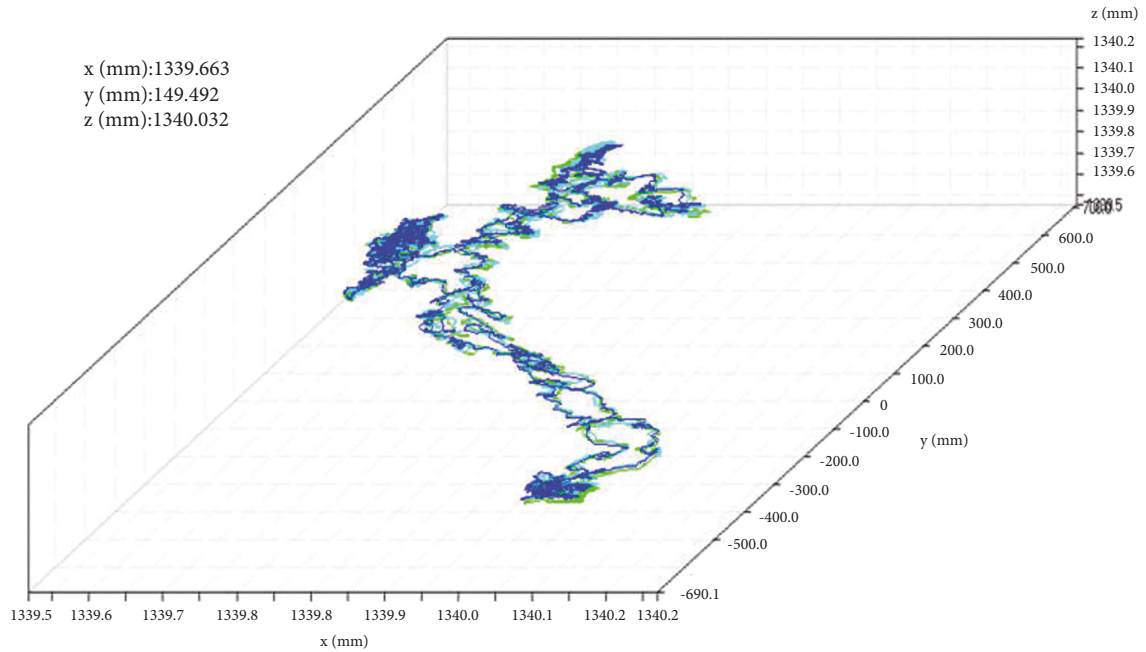
FIGURE 6: KR-3-R540 robot sensor layout.

and 7(b), it can be concluded that the pose accuracy of the robot's end effector is accurate after applying continuous excitation with the exciter. Serious deviation occurs. At this time, the robot state is regarded as a fault, and the specific fault is the fault at joint 1.

The specific content of the experiment includes the following steps: (1) Using the KR-3-R540 robot teach pendant, randomly set 10 closed-loop motion trajectories for the robot, and let the robot run at 30%, 50%, and 70% of the maximum speed. Complete the command movement, and the movement time is 20 s. (2) According to the above, set the robot joint fault; the fault status is divided into five categories; the first type of fault is expressed as no fault, the second type of fault is expressed as a joint fault, and the third type of fault is expressed as two joint faults, the fourth type of fault is represented as three joint faults, and the fifth type of fault is represented as four joint faults; the fault locations are set as joint 1, joint 2, joint 3, and joint 4. The detailed description of the fault is shown in Table 2. (3) Acceleration sensors are used to collect vibration signals of joints and end effectors in all working states of the robot. The sensors at the joints are single-term sensors, and the end-effectors are three-term sensors.



(a)



(b)

FIGURE 7: Comparison of the movement trajectories of the robot end effector before and after the exciter interference. (a) The motion trajectory of the robot end effector under normal conditions. (b) The exciter interferes with the movement trajectory of the robot end effector of joint 1.

4.2.2. *Experimental Data.* The joint vibration data of the robot is used to complete a series of steps to establish a fault diagnosis model suitable for the robot. Due to the limitation of technology and operation space, the acceleration sensor cannot be set inside the robot, but the sensor can only be set on the robot shell, which will inevitably collect the motion vibration signal and the robot resonance signal generated by the robot during the movement process. Filters need to be designed to eliminate these two interference signals. According to the modal analysis results, it can be known that

the motion frequency of the robot is about 100 Hz; the resonance frequency is about 2200 Hz.

In this study, the vibration data acquisition system under the LabVIEW platform was designed, and experiments were carried out on the gear fault simulation test bench, and the gear fault diagnosis data set under different working conditions was obtained. After the vibration signal is collected under all working states of the industrial robot, the corresponding experimental data are obtained, and a total of 150 sets of different experimental source data are

TABLE 2: Robot fault description.

Fault description	Type 1 fault	Type 2 fault	Type 3 fault	Type 4 fault	Type 5 fault
Joint 1	0	1	1	1	1
Joint 2	0	0	1	1	1
Joint 3	0	0	0	1	1
Joint 4	0	0	0	0	1

Note. "0" means there is no fault at the joint; "1" means there is a fault at the joint.

obtained. Each group includes the vibration signals of each joint and the end effector, a total of 1200 sets of sensor source data. First, filter the source data, and set the filter parameters as follows: the low-pass filter frequency is 100 Hz, and the high-pass filter frequency is 2200 Hz. Then, 1200 sets of source data are divided with 0.1s as the sample length, and 240000 experimental samples are obtained, of which the number of experimental samples in normal state is 48000, and the number of experimental samples in all five fault states is 192000. The vibration signal dataset of the robot is shown in Table 3.

## 5. Fault Diagnosis of Industrial Robot Based on Deep Belief Network

**5.1. Creation Process of Fault Diagnosis Model.** This section creates an industrial robot fault diagnosis model based on a deep belief network (DBN). First, the wavelet transform is used to decompose and reconstruct the vibration signal of the industrial robot joint and the end effector. Then, the energy entropy normalized eigenvector of the wavelet reconstructed signal is constructed using the information energy entropy and normalization theory. Finally, the normalized feature vector is divided into a training set and a test set. The training set is used for forward layer-by-layer training and reverse fine-tuning of the basic parameters of the fault diagnosis model. The test set is used to test the accuracy of the fault diagnosis model.

**5.2. Initialize DBN Network Parameters.** In the process of establishing a fault diagnosis model, it is necessary to initialize the basic parameters of the DBN network, including the number of layers of the DBN network model, the dimension of the underlying input sample, the dimension of the upper output label, and the forward unsupervised layer-by-layer training learning rate, inverse fine-tuning learning rate, number of iterations, momentum factor, and weight matrix and bias. Among these basic parameters, the number of model layers and the number of iterations can be set according to experience, mainly based on model training time and model accuracy; the underlying input sample dimension is determined by the number of elements of the energy entropy normalized feature vector. The label dimension is determined by the fault category labels contained in the sample data; the weight matrix, bias, learning rate, and momentum factor can be determined according to the following rules. (1) Initial setting of the weight matrix and bias: the initial setting of the weight matrix directly affects the training speed of the model. If the initial setting of the

connection weight is too large, the fault classification result will not meet the requirements, and the setting value is too small. This can lead to severely slow model training, neither of which is desirable. Usually, the initial setting of the weight should be a normal distribution conforming to  $N(0, 0.01)$ , and the initial setting of the bias between the visible layer and the hidden layer can be 0. Because in the process of DBN network training, the weight matrix and bias will be continuously updated according to the update criterion, which can be initialized according to the empirical formula. The empirical formula is expressed as follows:

$$\begin{aligned} w &= 0.1 \times \text{randn}(n, m), \\ a &= \text{zeros}(1, n), \\ b &= \text{zeros}(1, m). \end{aligned} \quad (1)$$

In the formula,  $n$  is the number of input layer neuron units and  $m$  is the number of output layer neuron units.

(2) Initial setting of learning rate: the learning rate is a key parameter of the gradient descent algorithm, an important basic algorithm in the DBN network training process, which determines the gradient descent distance each time the algorithm is executed. If the initial set value of the learning rate is relatively small, it will cause the model to step too slowly towards the minimum loss function value, which will take extra time to complete the model training; if the initial set value is large, it will lead to DBN. The reconstruction error of the network is too large, which will seriously cause model training failure. The initial setting of the forward unsupervised layer-by-layer training learning rate of the DBN model is generally 0.1, and the initial setting of the reverse fine-tuning learning rate is generally 0.01.

(3) Initialization of momentum factor: the main role of momentum factor in DBN model training is to improve the antioscillation performance of the training process by introducing the estimated gradient value after the previous iteration into the algorithm so that the algorithm can converge quickly and stably to the allowable range.

$$\begin{aligned} \theta_{t+1} &= \theta_t + \Delta\theta_t, \\ \Delta\theta_t &= m_b \Delta\theta_{t-1} + \varepsilon \times \frac{\partial \ln L}{\partial \ln \theta}. \end{aligned} \quad (2)$$

In the formula,  $m_b$  is momentum factor;  $\varepsilon$  is learning rate; and  $\partial \ln L / \partial \ln \theta$  is sample gradient.

The formula is the parameter update formula of the DBN network after adding the momentum factor. After the momentum factor is introduced, the update value of the DBN network parameter is calculated by the sample gradient

TABLE 3: Robot vibration signal dataset.

Running speed	Type 1 fault	Type 2 fault	Type 3 fault	Type 4 fault	Type 5 fault
30%	16000	16000	16000	16000	80000
50%	16000	16000	16000	16000	80000
70%	16000	16000	16000	16000	80000
Total	48000	48000	48000	48000	24000

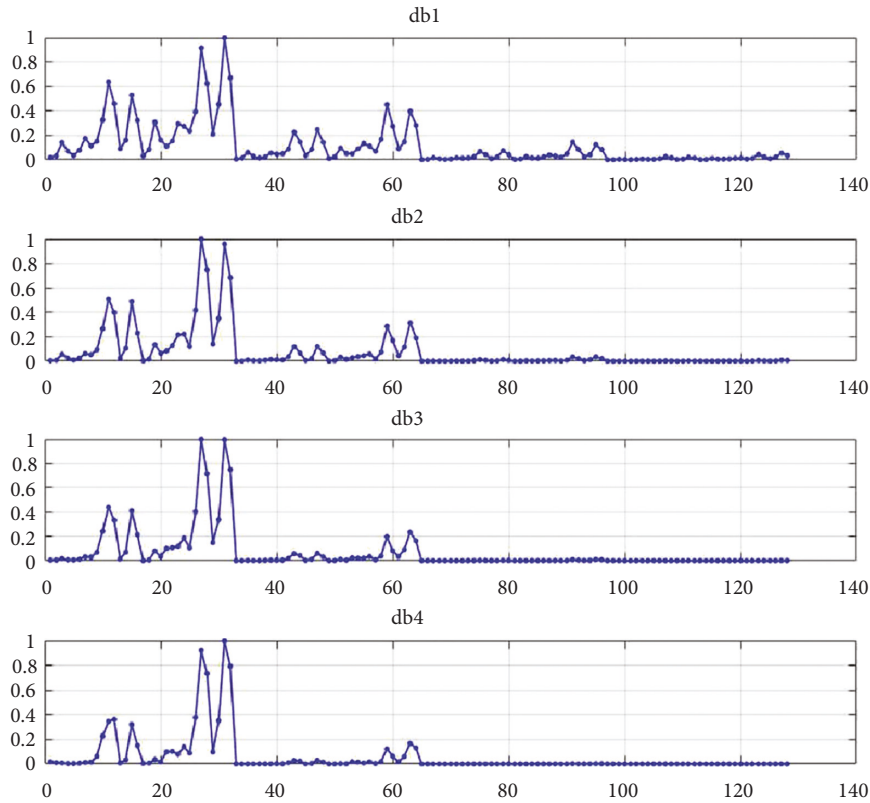


FIGURE 8: Node energy entropy under different wavelet bases. (a) db1. (b) db2. (c) db3. (d) db4.

and the correction value after the last iteration. The initial value of the momentum factor is generally set to  $[0.5, 0.9]$ .

**5.3. Model Accuracy Analysis.** According to the analysis, it can be determined that the number of wavelet envelopes is 7. Figure 8 shows the energy entropy normalized eigenvectors corresponding to different wavelet base numbers. The abscissa is the wavelet packet decomposition node, and the ordinate is the element value in the energy entropy normalized eigenvector. It can be seen from the comparison in the figure that when the wavelet base is db1, there are still obvious differences after the 96th node, and the signal information is relatively complete; when the wavelet base is greater than db1, especially when the wavelet base is above db4, at 96. The normalized energy entropy of all nodes after the node is close to 0, the difference between the nodes is very small, and the signal information is seriously lost. In order to make the normalized energy entropy feature vector have a good representation and meet the requirements of the underlying input of the DBN model, the wavelet base is selected as db1 in this paper.

The software used in this section is MATLAB 2019b, the operating system is Windows 10, the CPU is Intel Core i7, the graphics card is NVIDIA 930 M, and the running memory is 8 G. Divide the sample data into training set and test set according to the ratio of 4:1. The training set includes 192,000 experimental samples (38,400 normal experimental samples and 38,400 each of 4 types of fault experimental samples); the test set contains 48,000 experimental samples (9,600 normal experimental samples and 9,600 each of 4 types of fault experimental samples). According to the decomposition level of 7 and the wavelet base of db1, the wavelet packet is decomposed and normalized. Each experimental sample can construct an energy entropy normalized feature vector containing 128 elements. The training set of the DBN network model is 192,000 input samples, and the test set is 48,000 input samples. The input layer item of the DBN network model is 128, the output layer is represented as the sample fault label, and the output layer item is 6. The basic parameters of the DBN model are shown in Table 4, and the sample labels corresponding to the output layer are shown in Table 5. The number of iterations of the

TABLE 4: DBN model parameters.

Parameter	Numerical value
Wavelet packet decomposition layers	7
Wavelet packet wavelet basis	db1
Initial bias	0
Initial weight	0.001
Learning rate	0.1
Momentum factor	0.9
Input layer item	128
Output layer project	6

TABLE 5: Sample labels corresponding to the output layer.

Sample description	Sample label					
Class I failure	0	0	0	0	0	0
Type II fault	1	0	0	0	0	0
Three types of faults	1	1	0	0	0	0
Four types of faults	1	1	1	0	0	0
Five types of faults	1	1	1	1	0	0

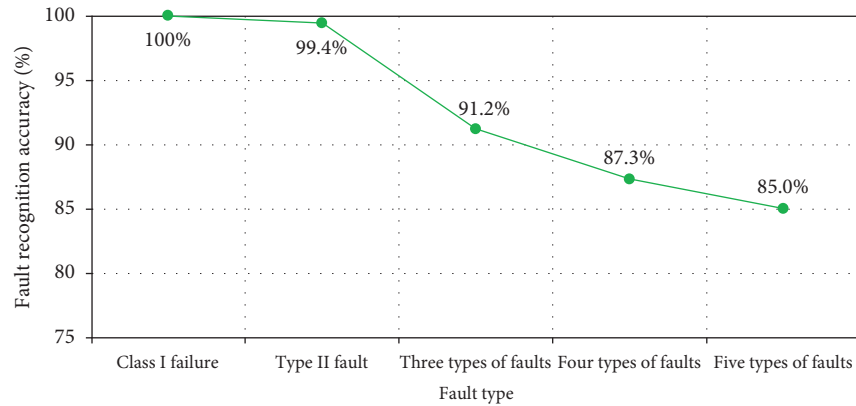


FIGURE 9: The fault identification accuracy of the fault diagnosis model based on DBN network when dealing with different fault states.

DBN model is set to 100, the number of inverse tuning times is preset to 100 and multiplied to 1000, and the learning rate and momentum factors are set to 0.1 and 0.9, respectively. Figure 9 shows the fault identification accuracy under different tuning times. It can be seen from Figure 9 that when the number of iterations reaches more than 900, the fault identification accuracy tends to a fixed value of 99.4%. It can be seen that the number of forward iterations of the DBN model used in this paper is 100 times, and the number of reverse tuning times is 100 times, should not be less than 900 times.

Figure 10 shows the fault identification accuracy of the fault diagnosis model based on DBN network when dealing with different fault states. It can be seen from the figure that the fault identification accuracy of the fault diagnosis model based on the DBN network can reach 99.4% when dealing with a single fault, and with the increase of the number of faults, the fault identification accuracy of the model also begins to decline, especially when dealing with the first fault. When there are five types of faults, the fault recognition accuracy is only about 85%. It is concluded that the fault

diagnosis model based on DBN network used in this chapter is not good in dealing with the fault diagnosis of multiple faults coexisting, and the model needs to be further improved.

## 6. Conclusion

The status of industrial robots in industrial production is getting higher and higher, and its normal operation is directly related to production safety, and it is also particularly important for the fault diagnosis of industrial robots. In order to improve the fault recognition accuracy of the industrial robot fault diagnosis model, this paper is based on the DSMT theory, and the results of the DBN network model diagnosis are fused at the decision level to achieve the purpose of improving the fault recognition accuracy of the model. Taking the output layer of the fault diagnosis model of the DBN network as the fault evidence, the conflict between the pieces of evidence is analyzed, the fusion rules and decision rules of DSMT are selected, and the fault diagnosis model based on DBN and DSMT is established. According to the requirements of the model for the experimental sample data, an experimental platform is built, the basic

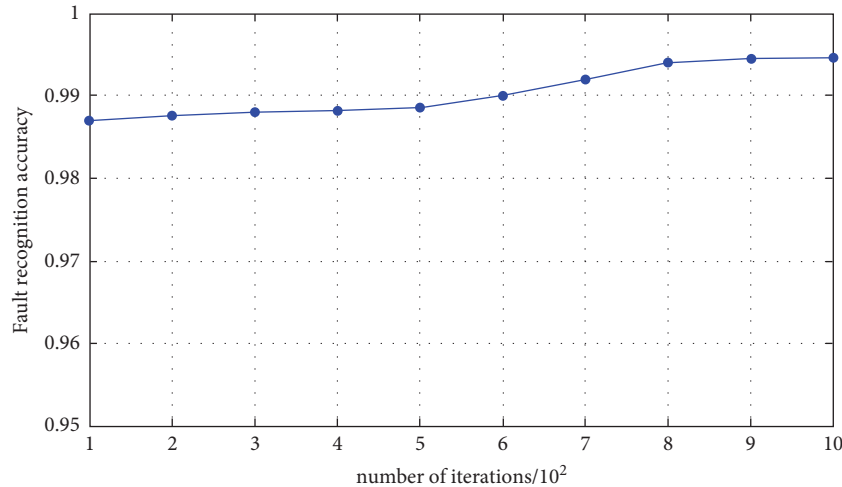


FIGURE 10: Fault recognition rate under different tuning times.

parameters of the DBN fault diagnosis model are determined through MATLAB programming, and a fault diagnosis model suitable for robots is established; finally, the fault diagnosis used in this experiment is verified by design experiments. The applicability of the model: It can be seen that the fault recognition accuracy of the industrial robot fault diagnosis model based on the DBN network can reach 99.4% when dealing with a single industrial robot fault. With the increase of the number of industrial robot faults, the industrial robot fault recognition accuracy of the model also begins to decline. Especially when dealing with the fifth type of fault, the accuracy of industrial robot fault recognition is only about 85%.

### Data Availability

The dataset can be accessed upon request from the corresponding author.

### Conflicts of Interest

The author declares that there are no conflicts of interest regarding the publication of this paper.

### Acknowledgments

This work was financially supported by funding for the Sixth Phase of Jiangsu 333 Project High-Level Talent Training Plan and Huai'an Natural Science Foundation Project (HABZ201920).

### References

- [1] W. A. C.B, H.H.K, and T.C.Y, "Use of an expert system shell to develop a power plant simulator for monitoring and fault diagnosis[J]," *Elsevier*, vol. 29, no. 1, pp. 27–33, 1994.
- [2] M. Burth and D. Filbert, "fault diagnosis of universal motors during run-down by nonlinear signal processing," *IFAC Proceedings Volumes*, vol. 30, no. 18, pp. 411–416, 1997.
- [3] A. Abdi, M. B. Tahoori, and E. S. Emamian, "fault diagnosis engineering of digital circuits can identify vulnerable molecules in complex cellular pathways[J]," *Science Signaling*, vol. 1, no. 42, p. 10, 2008.
- [4] H. Çaliş, A. Çakir, and E. Dandil, "Artificial immunity-based induction motor bearing fault diagnosis[J]," *Turkish Journal of Electrical Engineering and Computer Sciences*, vol. 21, no. 1, pp. 1–25, 2013.
- [5] P. Freeman, R. Pandita, N. Srivastava, and G. J. Balas, "Model-based and data-driven fault detection performance for a small UAV," *IEEE*, vol. 18, no. 4, pp. 1300–1309, 2013.
- [6] S. G. Liu, "Model-based fault detection of Modular and Reconfigurable Robots with joint torque sensing[J]," in *Proceedings of the 2013 IEEE/ASME International Conference on Advanced Intelligent Mechatronics*, vol. 1, pp. 134–139, Wollongong, NSW, Australia, 2013.
- [7] T. N. S. W M H, "Study on model-based fault detection and diagnosis for mobile robot: fault diagnosis of internal sensor and robot-localization[C]," in *Proceedings of the JSME annual Conference on Robotics and Mechatronics (Robomec)*, vol. 1, pp. 255–256, 2003.
- [8] A. K. S. Jardine, D. Lin, and D. Banjevic, "A review on machinery diagnostics and prognostics implementing condition-based maintenance," *Mechanical Systems and Signal Processing*, vol. 20, no. 7, pp. 1483–1510, 2006.
- [9] R. Yan and R. X. Gao, "Harmonic wavelet-based data filtering for enhanced machine defect identification," *Journal of Sound and Vibration*, vol. 329, no. 15, pp. 3203–3217, 2010.
- [10] Y. Lei, M. J. Zuo, Z. He, and Y. Zi, "A multidimensional hybrid intelligent method for gear fault diagnosis," *Expert Systems with Applications*, vol. 37, no. 2, pp. 1419–1430, 2010.
- [11] K. He, X. Zhang, and S. Ren, "Deep residual learning for image recognition," in *Proceedings of the The IEEE Conference on Computer Vision and Pattern Recognition*, IEEE, Las Vegas, USA, 2016.
- [12] A. Krizhevsky, I. Sutskever, and G. E. Hinton, "ImageNet classification with deep convolutional neural networks," *Communications of the ACM*, vol. 60, no. 6, pp. 84–90, New York, 2017.
- [13] H. Shao, H. Jiang, F. Wang, and Y. Wang, "Rolling bearing fault diagnosis using adaptive deep belief network with dual-tree complex wavelet packet," *ISA Transactions*, vol. 69, pp. 187–201, 2017.

- [14] M. Zhao, M. Kang, B. Tang, and M. Pecht, "Deep residual networks with dynamically weighted wavelet coefficients for fault diagnosis of planetary gearboxes," *IEEE Transactions on Industrial Electronics*, vol. 65, no. 5, pp. 4290–4300, 2018.
- [15] W. Sun, B. Yao, N. Zeng et al., "An intelligent gear fault diagnosis methodology using a complex wavelet enhanced convolutional neural network," *Materials*, vol. 10, no. 7, p. 790, 2017.
- [16] V. T. Tran, F. AlThobiani, and A. Ball, "An approach to fault diagnosis of reciprocating compressor valves using Teager-Kaiser energy operator and deep belief networks," *Expert Systems with Applications*, vol. 41, no. 9, pp. 4113–4122, 2014.
- [17] F. Jia, Y. Lei, J. Lin, X. Zhou, and N. Lu, "Deep neural networks: a promising tool for fault characteristic mining and intelligent diagnosis of rotating machinery with massive data," *Mechanical Systems and Signal Processing*, vol. 72-73, pp. 303–315, 2016.
- [18] H. Jeong, S. Park, S. Woo, and S. Lee, "Rotating machinery diagnostics using deep learning on orbit plot images," *Procedia Manufacturing*, vol. 5, pp. 1107–1118, 2016.
- [19] O. Obst, "Distributed fault detection in sensor networks using a recurrent neural network," *Neural Processing Letters*, vol. 40, no. 3, pp. 261–273, 2014.
- [20] O. Janssens, V. Slavkovicj, B. Vervisch et al., "Convolutional neural network based fault detection for rotating machinery," *Journal of Sound and Vibration*, vol. 377, pp. 331–345, 2016.
- [21] A. M. Abdel-Zaher and A. M. Eldeib, "Breast cancer classification using deep belief networks," *Expert Systems with Applications*, vol. 46, pp. 139–144, 2016.